



**PEDRO MIGUEL MARTINS BOTELHO**  
BSc in ⟨Mechanical Engineering Sciences⟩

**CONTROL AND OPTIMIZATION OF  
HIGH-PRESSURE COMPRESSOR BLADE  
DIMENSIONS AND CLEARANCES**

**INTRODUÇÃO À DISSERTAÇÃO**

MASTER IN MECHANICAL ENGINEERING  
NOVA University Lisbon  
⟨february⟩, ⟨2025⟩



**NOVA**

NOVA SCHOOL OF  
SCIENCE & TECHNOLOGY

DEPARTMENT OF  
MECHANICAL AND INDUSTRIAL ENGINEER-  
ING

# CONTROL AND OPTIMIZATION OF HIGH-PRESSURE COMPRESSOR BLADE DIMENSIONS AND CLEARANCES

## INTRODUÇÃO À DISSERTAÇÃO

**PEDRO MIGUEL MARTINS BOTELHO**

BSc in ⟨Mechanical Engineering Sciences⟩

**Adviser:** João Fradinho

*Assistant Professor, NOVA University Lisbon*

MASTER IN MECHANICAL ENGINEERING

NOVA University Lisbon  
⟨february⟩, ⟨2025⟩

# **Control and Optimization of High-Pressure Compressor Blade Dimensions and Clearances**

Copyright © Pedro Miguel Martins Botelho, NOVA School of Science and Technology, NOVA University Lisbon.

The NOVA School of Science and Technology and the NOVA University Lisbon have the right, perpetual and without geographical boundaries, to file and publish this dissertation through printed copies reproduced on paper or on digital form, or by any other means known or that may be invented, and to disseminate through scientific repositories and admit its copying and distribution for non-commercial, educational or research purposes, as long as credit is given to the author and editor.

# Contents

<b>List of Figures</b>	<b>v</b>
<b>List of Tables</b>	<b>vi</b>
<b>Acronyms</b>	<b>viii</b>
<b>1 Introduction</b>	<b>1</b>
1.1 Motivation . . . . .	1
1.2 Objectives . . . . .	2
<b>2 Company and LEAP-1A Overview</b>	<b>3</b>
2.1 TAP M&E . . . . .	3
2.2 LEAP Engine . . . . .	4
2.2.1 Turbofan . . . . .	4
2.2.2 LEAP Family . . . . .	6
2.2.3 LEAP-1A . . . . .	7
<b>3 Compressor</b>	<b>12</b>
3.1 Axial Compressor . . . . .	12
3.2 Blisks vs Bladed disks . . . . .	14
3.3 Rotor Blades . . . . .	15
3.4 Degradation Mechanisms of Compressor Blades . . . . .	17
<b>4 Dimensional Inspection and Measurement Equipment</b>	<b>19</b>
4.1 Available Measurement Equipment . . . . .	19
4.1.1 Creaform HandySCAN 3D scanner . . . . .	19
4.1.2 Mitutoyo Euro-C 121210 . . . . .	20
4.2 TAP ME: Previous Theses on Dimensional Inspection . . . . .	22
<b>5 Current Progress and Work Plan</b>	<b>23</b>
5.1 Work Plan . . . . .	24



# List of Figures

2.1 TurboJet Engine Work Cycle stages.[7] . . . . .	4
2.2 Turbofan Engine. [1] . . . . .	6
2.3 Leading Edge Aviation Propulsion (LEAP) Family.[2] . . . . .	6
2.4 LEAP-1A.[2] . . . . .	7
2.5 LEAP-1A Major Modules.[6] . . . . .	8
2.6 LEAP-1A fan blades vs CFM56 fan blades.[11] . . . . .	8
2.7 High and Low pressure rotors [11] . . . . .	10
2.8 Low Pressure Turbine (LPT). [11] . . . . .	10
2.9 Axial Compressor vs Turbine flow [15] . . . . .	11
2.10 LEAP-1A Accessory Drives.[11] . . . . .	11
3.1 Specific Consumption.[7] . . . . .	12
3.2 LEAP-1A HPC.[11] . . . . .	13
3.3 Axial Compressor Diagram and Pressure/Velocity Distribution.[7] . . . . .	14
3.4 LEAP-1A HPC. [11] . . . . .	15
3.5 Axial Fixing on the left and circumferential on the right.[7] . . . . .	16
3.6 Stage 6 Blade Dimension Check.[11] . . . . .	17
3.7 The effect on erosion trough time on the leading edge of a compressor blade [14] . . . . .	18
3.8 Comparison of thrust-specific fuel consumption (TSFC) between eroded and new compressor blades.[14] . . . . .	18
4.1 Mitutoyo Euro-C 121210 Components [14] . . . . .	21
4.2 DOF of the Renishaw probe [13] . . . . .	21
5.1 Process overview of blade maintenance cycle . . . . .	23
5.2 Work Plan. . . . .	24

## List of Tables

2.1	Transportes Aéreos Portugueses (TAP) Air Fleet Composition [3] . . . . .	3
2.2	Characteristics of the LEAP-1A engine.[4] . . . . .	7
2.3	Number of blades per stage on HPC [11] . . . . .	9
4.1	Renishaw probes available at TAP . . . . .	20



## Acronyms

<b>CAD</b>	Computer-Aided Design <a href="#">20</a>
<b>CFMI</b>	CFM International <a href="#">3</a>
<b>CL</b>	Chord Length <a href="#">21</a>
<b>CMM</b>	Coordinate Measuring Machine <a href="#">1, 20, 21, 23</a>
<b>EGT</b>	Exhaust gas temperature <a href="#">23</a>
<b>FOD</b>	Foreign Object Damage <a href="#">17</a>
<b>HP</b>	High Pressure <a href="#">5, 9</a>
<b>HPC</b>	High Pressure Compressor <a href="#">1, 9, 12–15, 18, 20, 23</a>
<b>HPT</b>	High Pressure Turbine <a href="#">9</a>
<b>LEAP</b>	Leading Edge Aviation Propulsion <a href="#">v, vi, 1, 3, 4, 6–8, 12–16, 23</a>
<b>LET</b>	Leading Edge Thickness <a href="#">21</a>
<b>LP</b>	Low Pressure <a href="#">5, 7–10</a>
<b>LPC</b>	Low Pressure Compressor <a href="#">8, 9, 13</a>
<b>LPT</b>	Low Pressure Turbine <a href="#">v, 9, 10</a>
<b>ME</b>	Maintenance and Engineering <a href="#">3, 19, 22</a>
<b>MM</b>	Major Module <a href="#">9</a>
<b>MRO</b>	Maintenance, Repair, and Overhaul <a href="#">3</a>
<b>RTM</b>	Resin Transfer Molding <a href="#">8</a>
<b>SB</b>	Service Bulletin <a href="#">1</a>
<b>TAP</b>	Transportes Aéreos Portugueses <a href="#">vi, 1, 3, 6, 19, 22</a>
<b>TET</b>	Trailing Edge Thickness <a href="#">21</a>



# Introduction

## 1.1 Motivation

In 2016, CFMI launched the LEAP-1A engine, ushering in a new era of efficiency and performance for commercial aviation. This engine builds on the solid foundation laid by the CFM56, which has been one of the most trusted and widely used engines in the industry.

Over the course of its life, an engine undergoes numerous upgrades and refinements aimed at improving its performance and fuel efficiency. These improvements often focus on precise measurements and dimensional control, as well as maintenance standards that ensure the engine continues to run smoothly and reliably. By implementing these updates, the engine can perform at its best throughout its service life, maximizing efficiency and reducing operational costs. Additionally, these advancements are aligned with the growing need for more sustainable aviation technologies, helping to meet the industry's environmental goals.

Each time an engine manufacturer introduces an optimization, it is implemented through a [Service Bulletin \(SB\)](#), a document that communicates details of modifications that can be made to the aircraft.

In recent years, two students, Edgar Farinhas and Pedro Rendas, explored a method for measuring the rotor blade dimensions of the [High Pressure Compressor \(HPC\)](#) using a [Coordinate Measuring Machine \(CMM\)](#) machine, focusing specifically on the blades of the CFM56 HPC. [5]

Since it entered service, [TAP](#) has integrated the [LEAP-1A](#) into approximately half of its fleet, replacing the CFM56. As the performance of the [HPC](#) directly influences engine efficiency and overall operational effectiveness, establishing robust monitoring and control measures has become a critical priority, alongside investigating the factors that affect its performance.

## 1.2 Objectives

Various factors influence engine performance, and the high-pressure compressor (HPC) plays a key role in this. The efficiency of the HPC is largely determined by the design of its rotor blades, which operate under intense aerodynamic and thermal conditions. This directly impacts the engine's performance and fuel consumption. Despite their importance, TAP has no standardized dimensional inspection process for these components.

Using the available equipment at the TAP Engine Shop, including the 3D scanner and Coordinate Measuring Machine (CMM), this study aims to develop a practical and efficient method for measuring the chord length of HPC blades, as this parameter is crucial in assessing blade wear and its correlation with engine performance in test cell conditions. Additionally, the study seeks to create a tool to measure the total clearance of the entire stage after assembly, optimizing the assembly process and making it more efficient.

An important objective is to control the platform gap of the blades during their preparation for assembly, developing a tool capable of accurately simulating the blade fit. This will enable the immediate determination of the required number of wide and narrow platform blades, making the process faster and more efficient—an important consideration for TAP's operational needs.

By establishing this methodology, it will be possible to correlate these geometric characteristics with engine performance as tested in the test cell. Understanding these relationships will help optimize maintenance procedures and improve overall efficiency. This thesis represents an important step toward implementing a more advanced dimensional inspection process at TAP, contributing to the company's ongoing efforts to enhance engine performance and reliability.

## Company and LEAP-1A Overview

### 2.1 TAP M&E

**TAP** was founded in 1945, during the end of World War II, a period marked by significant development in the aviation industry.

**TAP Maintenance and Engineering (ME)** is responsible for performing maintenance and engineering support services to **TAP**'s airline fleet and third-party customers. Services such as Aircraft Maintenance, Engine Repair and Overhaul and Components Repair and Overhaul.

To maintain **TAP** Air Portugal's reputation as one of the most reliable airlines in the world, **TAP ME** embraces the concept of *Care2Quality*. This philosophy is founded on three key pillars: **Safety**, **Quality**, and **Relationships**. It is integrated across all **TAP ME** products and services, which are organized into five main departments: *Care2Airframe*, *Care2Engines*, *Care2Components*, *Care2Engineering*, and *Care2Technical Labs*.

**TAP ME** offers extensive **Maintenance, Repair, and Overhaul (MRO)** services for a variety of aircraft systems and engine models. For **CFM International (CFMI)** engines, including the CFM56 series and **LEAP-1A**, it provides light and heavy maintenance, engine testing, troubleshooting, redelivery checks, technical consulting, and engine trend monitoring.

Currently in its fleet **TAP** has the following aircraft:

Table 2.1: **TAP** Air Fleet Composition [3]

Aircraft	Active N°	Age
Airbus A319ceo	3	23
Airbus A320ceo	15	19
Airbus A320neo	15	3
Airbus A321ceo	3	22
Airbus A321neo	12	4
Airbus A321LRneo	11	3
Airbus A330ceo	3	16
Airbus A330neo	19	5

## 2.2 LEAP Engine

LEAP engine family, developed and produced by CFM International—a joint venture between Safran Aircraft Engines and GE Aerospace—continues the legacy of the CFM56 as a best-seller in commercial aviation. Introduced in 2016, the LEAP powers the Airbus A320neo, Boeing 737 MAX, and COMAC C919, delivering a 15% improvement in fuel efficiency, along with reduced noise and emissions, while maintaining industry-leading reliability and cost-effectiveness. This advanced engine reflects the enduring success of the partnership between Safran and GE, which has been extended until 2050.

The LEAP, like most modern commercial aircraft engines, is a turbofan engine.

### 2.2.1 Turbofan

The Turbofan engine applies the same principle as the turbojet and all jet engines, Newton's third law: "For every action, there is an equal and opposite reaction". In this case, the first object is the engine itself and the second is the atmospheric air that is forced to accelerate as it passes through the engine causing the airplane to move forward.

To understand how the turbofan engine works, it is a good approach to analyze the turbojet working cycle and how it is processed first. As shown in Figure 2.1 the working cycle of a TurboJet has 4 main stages: Air intake, Compression, Combustion and Exhaust. At intake, the air is at atmospheric pressure, but as it passes through the compressors, it is compressed to optimal pressure and temperature conditions for combustion. Upon entering the combustion chamber, fuel nozzles mix the fuel and air, creating a homogeneous mixture that minimizes the peak temperature during combustion. During the combustion process, this mixture burns at constant pressure, increasing the air's volume while causing a decrease in pressure. The gases resulting from combustion expand through the turbine and jet pipe back to atmosphere providing the force needed to propel the airplane forward. During this part of the cycle, some of the energy in the expanding gases is turned into mechanical power by the turbine.

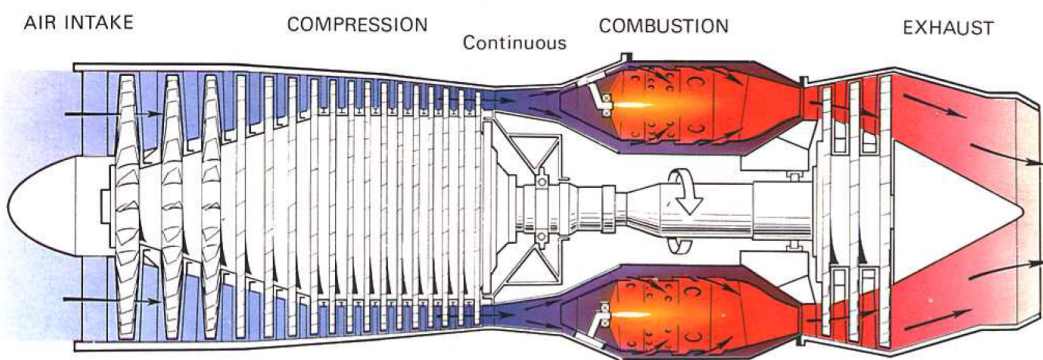


Figure 2.1: TurboJet Engine Work Cycle stages.[7]

Analysing the Turbofan work cycle requires a more complex approach since the air that goes through the combustor is now only responsible for 20% of the thrust power.

At the start, the engine's high-pressure shaft receives mechanical power with the assistance of a system called the Air Turbine Starter. This rotation drives the compressor blades, drawing air through the engine and initiating the compression process. The airflow through the engine also causes the fan to start moving. Once the engine reaches 20% of its maximum RPM, sufficient compression is generated to initiate combustion. With everything in motion, the engine enters a cycle similar to the turbojet working cycle. The gases produced from combustion expand through the **High Pressure (HP)** and **Low Pressure (LP)** turbines, delivering mechanical power to the **HP** and **LP** shafts. These shafts, in turn, transmit rotational energy to the **HP** and **LP** compressors as well as the front fan. As the fan rotates at high speed, it separates the incoming air into two distinct streams, forming the bypass ratio. Commercial aircraft engines, such as the LEAP-1A, are high-bypass ratio engines. In these engines, one stream of air enters the engine core, powering the turbojet-like working cycle. The remaining air, approximately 80% of the total intake, is channeled around the engine core. This bypassed air is directed into a narrow passage known as the fan duct, where its speed increases significantly. This accelerated airflow generates the majority of the thrust required to lift the aircraft.

In summary, the main differences between turbofan and turbojet engines lie in their airflow management and structural design. A key distinction is the large fan at the front of the turbofan, which directs a significant portion of the air around the engine core, defining the bypass ratio, which is the ratio of the amount of air bypassing the core to the amount of air passing through it, as illustrated in Figure 2.2. Weight wise, for the same power output, given the fact that all the high pressure rotating assemblies diameter can be reduced, the turbofan engines are lighter, improving the power-weight ratio of the engine. A low bypass ratio engine has a weight reduction of 20 percent compared to a pure jet engine for the same air mass flow.<sup>[7]</sup> Another significant advancement in turbofan engines is the introduction of the multi-spool or multi-shaft system, although this technology can also be applied to pure jet engines. The presence of both **LP** and **HP** turbines and compressors requires each assembly to rotate at different speeds, since just a percentage of the air that flows through the **LP** Compressor goes into the **HP** one (the majority of the air forms the bypass flow). This is essential for achieving higher efficiency, as each component operates at its optimal rotational velocity. Most commercial aircraft engines are high-bypass engines, and the typical configuration for these engines is a two-shaft system. As illustrated in Figure 2.2 the **LP** compressor is powered by a shaft coming from the **LP** turbine, and the same applies to the **HP** spool.

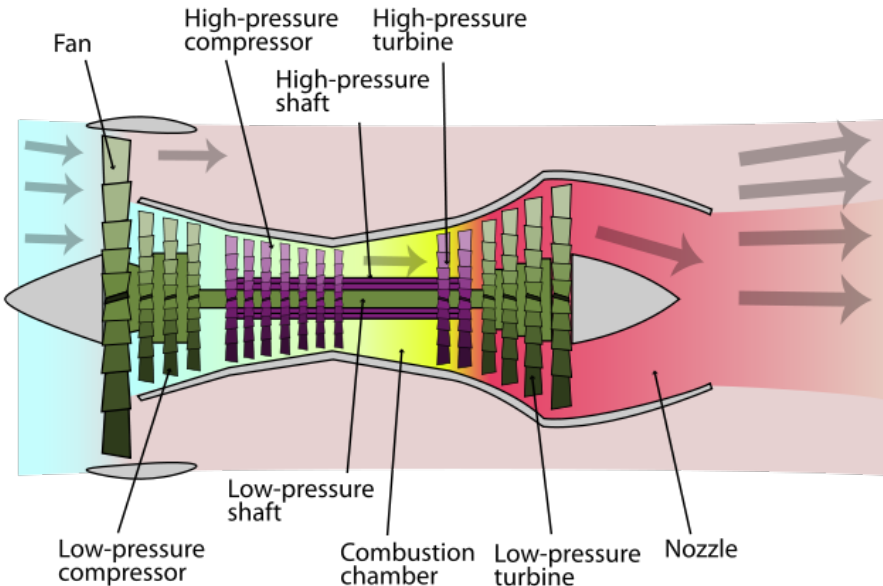


Figure 2.2: Turbofan Engine. [1]

### 2.2.2 LEAP Family

As mentioned at the beginning of this chapter, the LEAP engine powers a variety of aircraft, with its characteristics varying depending on the application. Therefore, we can categorize the LEAP engine family based on application and thrust power.

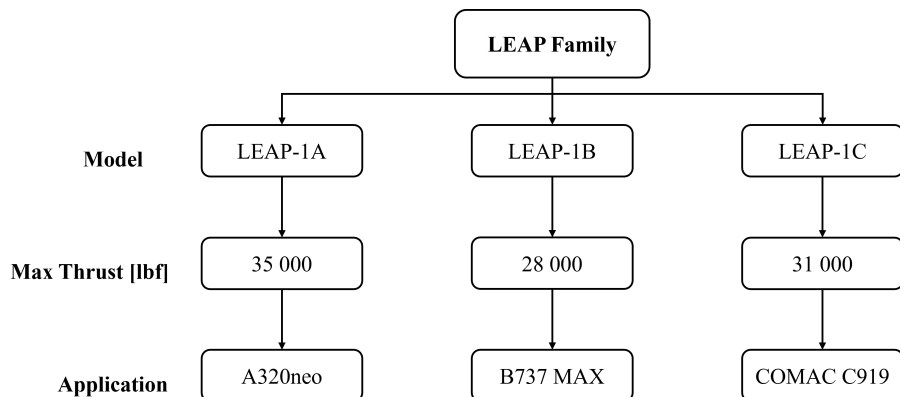


Figure 2.3: LEAP Family.[2]

Each model also has variations based on its thrust. For instance, the LEAP-1A can be further subcategorized into LEAP-1A23, LEAP-1A24, LEAP-1A26, LEAP-1A30, LEAP-1A32, LEAP-1A33, and LEAP-1A35. Considering that in 'LEAP-1A24', the '24' indicates the engine's thrust capacity of 24 klbf.

Currently, in the TAP Air Fleet Composition, the LEAP-1A26 and LEAP-1A32 engines are used respectively in the Airbus A320neo and A321neo.

### 2.2.3 LEAP-1A

The LEAP-1A, represented in Figure 2.4, is a high-bypass turbofan engine designed to power the next-generation Airbus A320neo. This section presents some of its key features, along with its main modules and innovations in comparison to its predecessor, the CFM56. Most of this information is derived from the engine's brochure and training manual.



Figure 2.4: LEAP-1A.[2]

This powerplant is presented with the following characteristics in Table 2.2.

Table 2.2: Characteristics of the LEAP-1A engine.[4]

Characteristic	Value
Takeoff thrust	Up to 35,000 lbf
Bypass ratio	11:1
Overall pressure ratio	40:1
Fan diameter	1.98 m (78 in)
Compressor stages (fan/booster/HPC)	1 + 3 + 10
Turbine stages (HP/LP)	2 + 7
Weight	3007 kg
Length	3.35 m (11 ft)
Width	2.53 m (8.3 ft)
Height	2.38 m (7.8 ft)

Design and function wise LEAP-1A present in its composition 4 Major modules. As represented in Figure 2.5, Fan and Booster, Core, LP Turbine and Accessory Drive Major Modules.

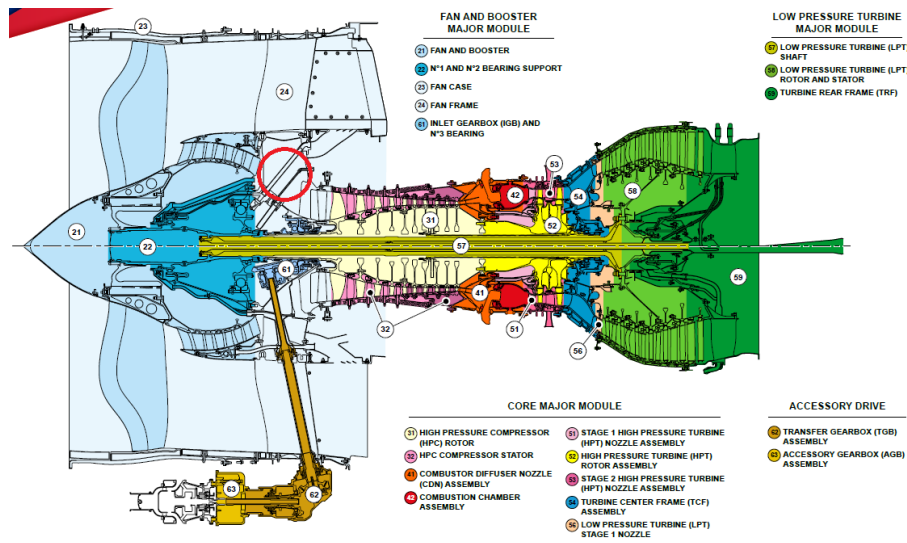


Figure 2.5: LEAP-1A Major Modules.[6]

### 2.2.3.1 Fan and Booster Major Module

As shown in Figure 2.5, the Fan and Booster Major Module consists of the Fan and Booster itself, two bearing supports, the fan case, the fan frame, the inlet gearbox, and the number 3 bearing.

The Fan and Booster assembly represents the integration of the front fan and the LP Compressor.

The fan itself is composed of a single assembly that includes one front spinner, 18 fan blades, a flow splitter, and a platform front shroud.

The Low Pressure Compressor (LPC) consists of three stages: the first stage has 62 blades, the second stage has 75 blades, and the third stage has 72 blades.

One of the major technological breakthroughs in the new LEAP-1A engine is the production of its fan blades. These blades are manufactured using additive manufacturing with 3D-woven Resin Transfer Molding (RTM) carbon fiber composites. Compared to the solid titanium blades of the CFM56, this advancement allows for larger blades, as illustrated in Figure 2.6, without increasing the engine's weight. According to the company, this material helps reduce engine weight by 500 lbs per unit.

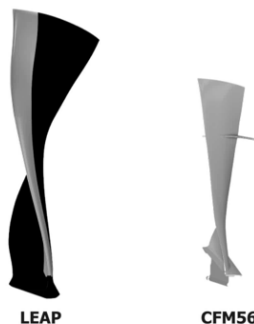


Figure 2.6: LEAP-1A fan blades vs CFM56 fan blades.[11]

In summary, the purpose of this engine assembly is to impart kinetic energy to the incoming airflow, separate the primary and secondary airflow, and expel the hot air generated by the engine.

### 2.2.3.2 Core

Next is the Core Major Module, which is responsible for generating thrust by producing power through highly compressed air.

This **Major Module (MM)** comprises the assembly of the **HPC**, combustion chamber, and **High Pressure Turbine (HPT)**. Additionally, it is divided into nine sub-modules.

The **HPC** consists of the HPC rotor and stator, while the **HPT** includes the HPT rotor along with the stage 1 and stage 2 nozzle assemblies. The Core Major Module also incorporates the Turbine Center Frame and the **LPT Stage 1 Nozzle**.

To achieve optimal performance, the **HPC** features 10 stages, as shown in Table 2.3. Each stage consists of one rotor and one stator. The first five stages of compression are achieved through blisks, while the remaining five stages use compressor blades with circumferential assembly. This mini module has the purpose of increasing the pressure of the booster discharge air for combustion.

Table 2.3: Number of blades per stage on HPC [11]

Stage	1	2	3	4	5	6	7	8	9	10
Number of blades	-	-	-	-	-	62+2+2	57+2+2	63+2+2	60+2+2	64+2+2

It is important to note that the HPC rotor is coupled with the HPT, as shown in Figure 2.7. This coupling allows the kinetic energy extracted from the HPT to be used for compressing the airflow. Likewise, the same principle applies to the **LPC** and **LPT**.

In Figure 2.7, the yellow assembly represents the Low-Pressure rotor, while the orange assembly corresponds to the High-Pressure rotor.

As mentioned in 2.2.1, these rotors rotate at different speeds. The **LP** rotor operates at N1 speed (3 850 RPM), whereas the **HP** rotor rotates at N2 speed (16 645 RPM).

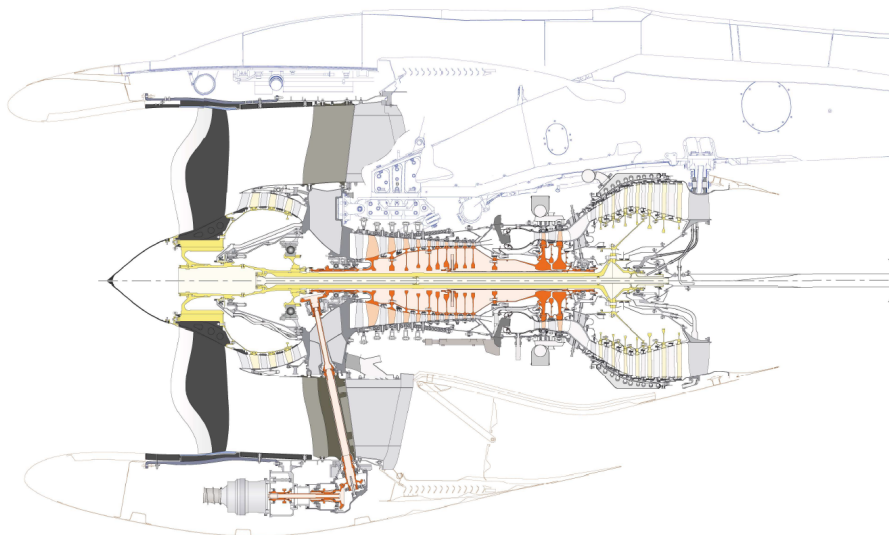


Figure 2.7: High and Low pressure rotors [11]

### 2.2.3.3 LP Turbine Major Module

The LP Turbine Major Module, represented in Figure 2.8, is composed by the LP turbine shaft, rotor and stator and the turbine rear frame.

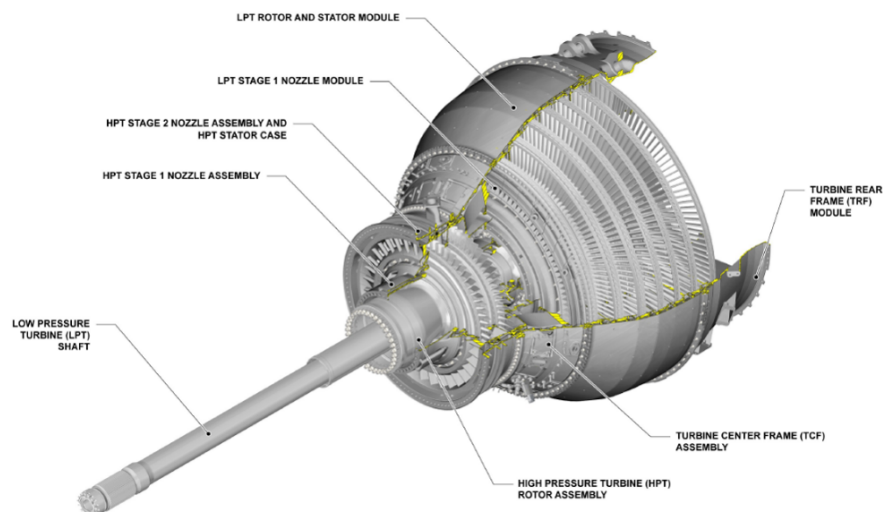


Figure 2.8: LPT. [11]

Its primary function is to supply mechanical power to the LP Compressor by converting the thermal energy from the hot gases released from the combustion chambers into kinetic energy while simultaneously decompressing it.

It is worth noting that while both turbines and compressors present similar designs and compositions, their functions are fundamentally opposite.

As previously mentioned, compressors consume energy and transfer it to the air, compressing it while increasing its velocity, whereas turbines absorb energy from the expansion of the combustion gases and convert it into mechanical power.

Both components consist of stages that include one stationary and one rotating element, but their purposes and arrangements differ. As illustrated in Figure 2.9, in a compressor, a rotor row is followed by a stationary vane row, while in a turbine, a stationary nozzle precedes a rotating rotor row. The stationary vanes in the compressor are responsible for further compressing the air through diffusion processes, whereas the nozzles in the turbine decompress the airflow and guide it in the most efficient direction, maximizing the kinetic energy absorbed by the turbine blades.

A more detailed explanation of the compressor's operation is provided in the following sections.

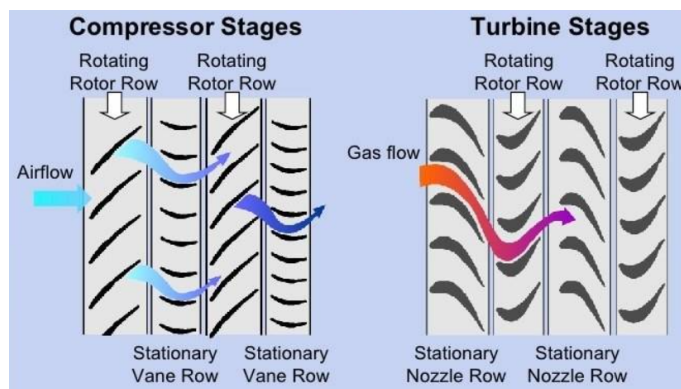


Figure 2.9: Axial Compressor vs Turbine flow [15]

#### 2.2.3.4 Accessory Drive

As shown in Figure 2.10, the accessory drive delivers torque to the HPC to initiate engine start-up, as described in 2.2.1, enabling the compression process (red arrow path). During the engine's operating cycle, it supplies mechanical energy to both the aircraft and engine accessories (orange arrow path).

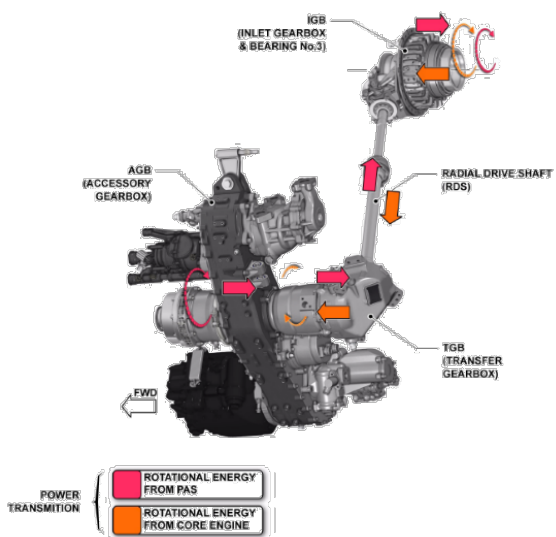


Figure 2.10: LEAP-1A Accessory Drives.[11]

# Compressor

Being the purpose of this thesis "*Control and Optimization of High-Pressure Compressor Blade Dimensions and Clearances,*" it is crucial to study the operation of engine compressors, understanding their working principles and the key criteria that must be considered in order to improve the blades dimensions and clearances in engine reliability and performance.

This section highlights the key criteria, provides an overview of the module's operation, and explains how compressor wear during the engine's operating cycle affects its performance.

## 3.1 Axial Compressor

In gas turbine engines, there are two primary types of compressors: axial and centrifugal flow compressors. Both are driven by a shaft connected to the turbine; however, the axial type is easier to manufacture and can be designed to achieve higher pressure ratios. For this reason, commercial turbofan engines typically utilize this type of compressor, specifically in the [LEAP-1A](#) engine.

Higher pressure ratios are proven to improve fuel consumption as shown on Figure 3.1

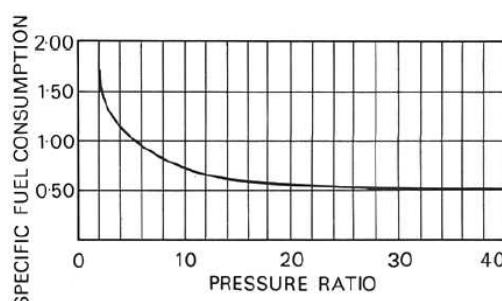


Figure 3.1: Specific Consumption.[\[7\]](#)

Using the [LEAP-1A HPC](#) as example, an axial compressor consists of one or more rotor assemblies which in turn can be one single part, representing a blisk, or a circumferential

### 3.1. AXIAL COMPRESSOR

blade assembly. These assemblies are mounted between the 2 bearing in a casing which incorporate the stator vanes.

As mentioned in the previous sections, this compressor is a twin-spool, multi-stage unit consisting of 3+10 stages.

In other words, the compressor is composed of the [LPC](#) with three stages, followed by the [HPC](#) with ten stages. Additionally, the front fan can also be considered part of the compression system, as it contributes to air compression despite not being its primary function, effectively serving as the first stage of the [LPC](#).

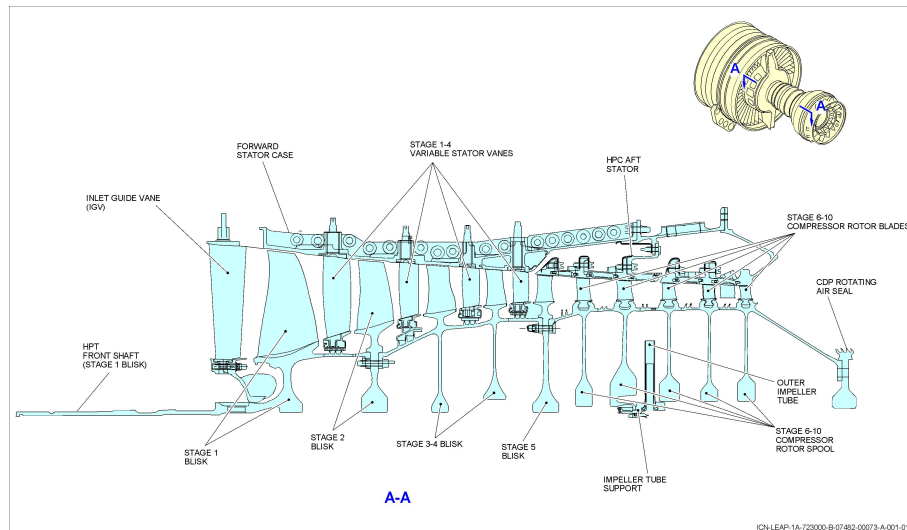


Figure 3.2: LEAP-1A HPC.[\[11\]](#)

With the engine running, the turbine transmits power to the compressor, driving it at high speed and ensuring a continuous airflow. As the air enters the [LPC](#), it passes through the first rotor, where the rotating airfoil-shaped blades transfer kinetic energy to the airflow by increasing its tangential momentum. Simultaneously, pressure rises with the aid of the diffusion process. Next the air flows into the vanes where kinetic energy increase is converted in pressure increase by the same process found in the rotational step.

The requirement for a high-pressure ratio on the shaft demands precise airflow control during engine operation to prevent airflow reversal, as a compressor inherently forces air from a low-pressure region to a higher-pressure zone. To achieve this, the guide vanes in the initial four stages functions as Variable Stator Vanes (VSV's), followed by fixed stator vanes in the subsequent stages. These variable vanes progressively close at lower airflow speeds to maintain an optimal air angle on the downstream rotor blades, preventing reverse flow and avoiding compressor stall.

During each stage the increase of pressure is relatively small as shown in Figure 3.3 in order to avoid air breakaway at the blades and subsequent blade stall. On another hand, the multi-stage process allows the [LEAP](#) to achieve an Overall Pressure ratio of 40:1. This ratio represents the Pressure ratio of all the engine not just the compressor.

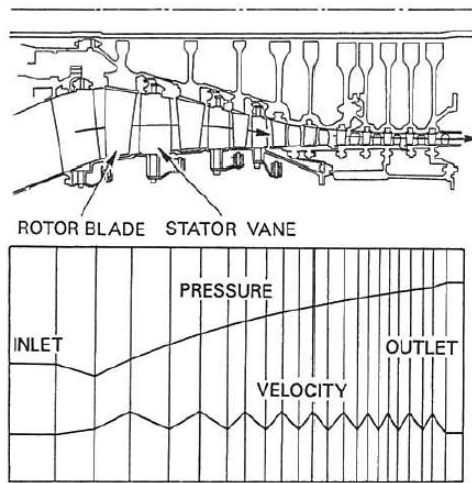


Figure 3.3: Axial Compressor Diagram and Pressure/Velocity Distribution.[\[7\]](#)

### 3.2 Blisks vs Bladed disks

In Figure 3.4, the HPC of the LEAP-1A engine is shown, consisting of five blisks, an impeller tube support, a five-stage rotor, and a rotating seal.

The incorporation of blisks in compressors represents a significant innovation in the LEAP-1A design compared to previous-generation turbofan engines. This advancement was introduced in aviation to enhance engine performance. Blisks significantly reduce rotor weight compared to conventional aero-engine disks. Since compressor and turbine disks contribute to over 20% of the engine's structural weight, their design presents numerous static and dynamic challenges.

From a design perspective, traditional bladed disks require the assembly of multiple components with different connection features, such as airfoil roots, disk roots, and locking mechanisms. In contrast, a blisk integrates all these elements into a single part, leading to several benefits:

- A reduction in the total number of parts, contributing to lower overall weight and faster assembly.
- Fewer contact surfaces, minimizing gaps where airflow could infiltrate and disrupt engine operation.
- Eliminates dovetails and its associated issues such as its weight and propensity for leakages.
- Simplified assembly during both production and maintenance, resulting in lower manufacturing costs and shorter lead times.

- The use of blisks imply bigger clearance between the blade tip and the stator which impacts engines performance.

However, blisks present significant drawbacks when compared to bladed disks, particularly in terms of maintenance and repairability. In the event of damage to an individual airfoil, the entire blisk must be replaced, leading to considerably higher costs than replacing a single blade. Additionally, as a single integrated component, the blisk eliminates the option of using different materials for the airfoil and the disk. The increased rigidity of the blisk also results in a lack of damping, which reduces its fatigue resistance.

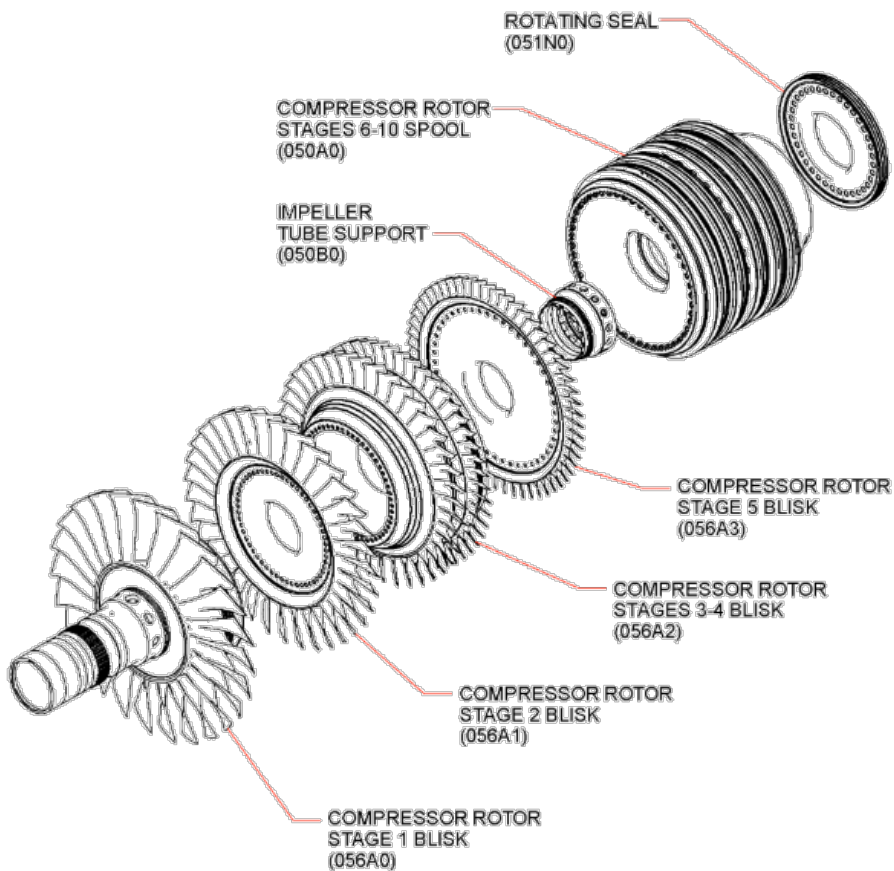


Figure 3.4: LEAP-1A HPC. [11]

### 3.3 Rotor Blades

As previously described, the **HPC** of the **LEAP-1A** consists of 10 stages, with the first five rotors designed as blisks and the last five as disks with fixed rotor blades. The attachment of these blades to the disk can be achieved through two different methods: axial or circumferential fixing, as illustrated in Figure 3.5.

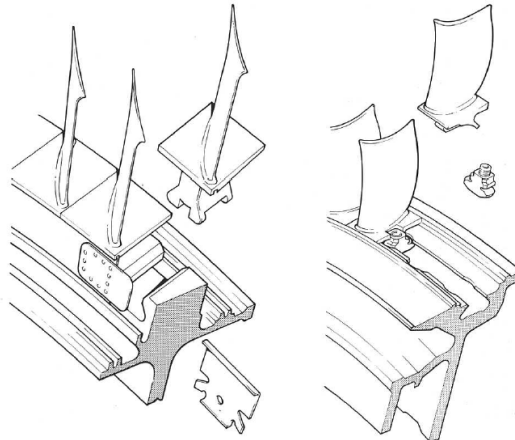


Figure 3.5: Axial Fixing on the left and circumferential on the right.[7]

The blades and disk shown in Figure 3.5 are not actual LEAP-1A components but merely illustrative examples.

The blades of the last five stages of the HPC are made from Inconel 718 and Inconel 718Plus. Inconel 718 is used in the first two stages, while Inconel 718Plus is used in stages 8, 9, and 10.

This material differs from the the blades found on the LPC or the blisks since with the increase of pressure temperature also rises.

INCONEL alloy 718 (UNS N07718/W.Nr. 2.4668) is a high-strength, corrosion-resistant nickel chromium material used at -252.78 to 704.44°C. [10]

Focusing on the last five stages of the HPC, in alignment with the objectives of this thesis, it is crucial to understand which dimensions impact the engine's performance, particularly as blade dimensions undergo changes due to excessive wear and usage, ultimately affecting engine performance and reliability.

TAP ME technicians are responsible for monitoring the most critical dimensions during the engine repair process.

These dimensions are specified in [11] and are illustrated in Figure 3.6. Based on this, the critical dimensions can be defined as follows: tip chord length (CH), blade tip length (H), leading edge thickness (TL), and trailing edge thickness (TU).

### 3.4. DEGRADATION MECHANISMS OF COMPRESSOR BLADES

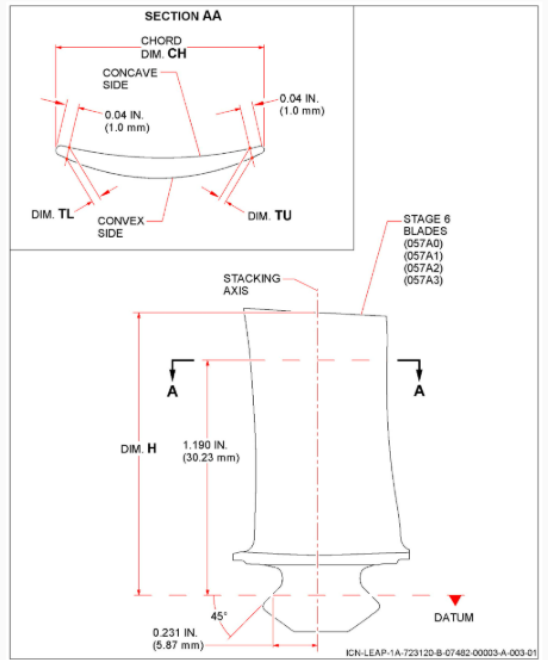


Figure 3.6: Stage 6 Blade Dimension Check.[11]

In each stage of the HPC, the blades can be categorized into three types: narrow body blades, wide body blades, and locking blades. The narrow and wide body blades are used to adjust the platform gaps, ensuring proper assembly and optimal aerodynamic performance. The locking blades, on the other hand, incorporate locking mechanisms that secure them in place, preventing movement during engine operation. The correct selection and placement of these blade types are essential to maintaining structural integrity and performance within the compressor. Therefore, ensuring the correct gap between the blades during the repair process is crucial to maintaining proper assembly, aerodynamic efficiency, and overall engine reliability.

## 3.4 Degradation Mechanisms of Compressor Blades

The degradation of compressor blades is a critical factor affecting engine performance and reliability. Commercial aircraft engines operate in diverse environments, exposing the engine core to various particles and contaminants.

These ingested particles, collectively known as **Foreign Object Damage (FOD)**, include sand, metal fragments, birds, and other debris. The ingestion of such contaminants has two main consequences: if the particle is a hardbody, it can cause direct erosion and structural damage to the blades, leading to dimensional loss. In contrast, if the particle is a softbody, such as a bird, it can obstruct airflow, causing performance degradation or even severe engine failure.

In particular, this section examines the impacts of FOD on the geometry of compressor blades. The ingestion of particles during the engine cycle can lead to a reduction in

blade chord, loss of blade thickness, alteration of the leading and trailing edge shapes, thinning of the blade trailing edge, blunting of the leading edge, and an increase in surface roughness.

Alterations in the blade geometry, such as changes in chord length, thickness loss, and alterations to the leading and trailing edges, result in increased clearance losses at the blade tips, higher frictional losses, and a significant reduction in off-idle and open beta stall margins. In Figure 3.7 its possible to observe the damages caused on the leading edge by continuous erosion. [14]

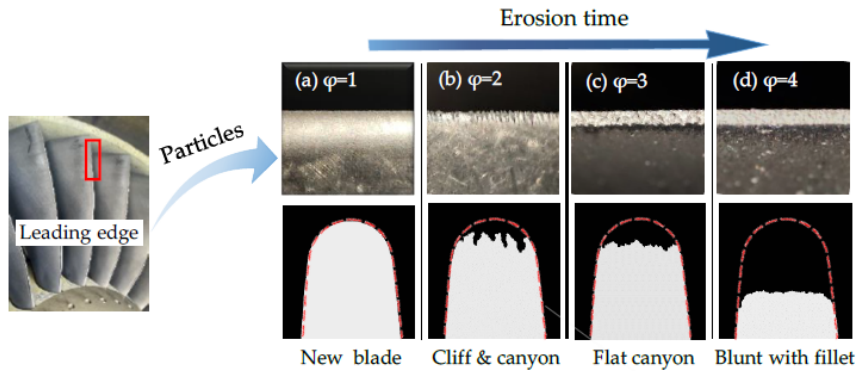


Figure 3.7: The effect on erosion trough time on the leading edge of a compressor blade [14]

These effects influence HPC efficiency and, consequently, engine performance. In particular, compressor blade erosion, coupled with efficiency losses throughout the engine, can increase fuel consumption by nearly 1 percent compared to new blades (see Figure 3.8) [14].

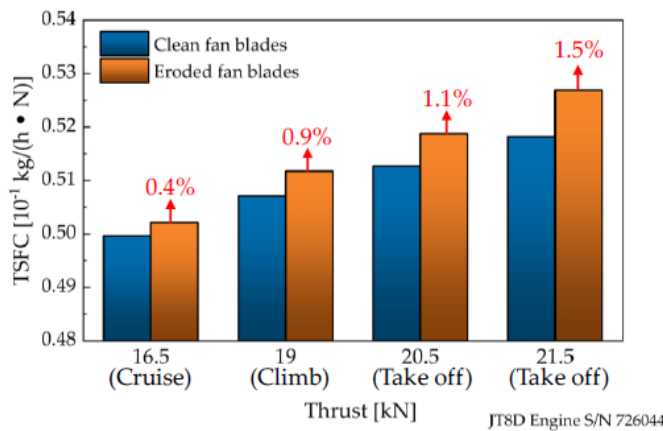


Figure 3.8: Comparison of thrust-specific fuel consumption (TSFC) between eroded and new compressor blades.[14]

# Dimensional Inspection and Measurement Equipment

This chapter introduces the equipment and methodology that can be used for dimensional inspection in engine component analysis. Keeping parts within the required tolerances is essential for ensuring performance and durability. A 3D scanner makes it possible to generate a digital model of the components, while a coordinate measuring machine (CMM) allows for precise measurement and comparison with nominal dimensions. These tools help improve the accuracy of the analysis and support potential optimization of the components at [TAP ME](#) Engine Shop.

The Engine Shop at [TAP ME](#) has a specialized Dimensional Inspection department responsible for verifying component dimensions in accordance with the manual, ensuring optimal engine performance and reliability.

## 4.1 Available Measurement Equipment

To ensure precise measurements, the department relies on advanced equipment, such as the Creaform HandySCAN 3D scanner, which captures highly accurate digital models of components, and the Mitutoyo Euro-C 121210 coordinate measuring machine (CMM), which provides detailed dimensional and geometric analysis. By using these tools, the team can carry out thorough inspections, verify tolerances, and explore opportunities for improving component performance.

### 4.1.1 Creaform HandySCAN 3D scanner

The HandySCAN 3D is a high-precision laser scanner developed by Creaform, designed for portable 3D scanning of objects with complex geometries. It uses laser triangulation to capture detailed 3D models with high accuracy and resolution. It presents the following technical data:

- **Accuracy:** 0.025 mm (0.0009 in)

- **Volumetric Accuracy:** Up to 0.020 mm + 0.015 mm/m
- **Light Source:** 22–30 blue laser lines
- **Working Distance:** 200 to 750 mm
- **Recommended Part Size Range:** 0.05 – 4 m
- **Weight:** 0.94 kg

The HandySCAN 3D laser scanner is used in conjunction with VXelements, an integrated 3D software platform that allows real-time data acquisition, post-processing, and analysis.

During the development of this thesis, this equipment will enable the practice of reverse engineering. Using the HandySCAN 3D scanner, detailed physical data from the HPC blades can be captured, and with the VXelements software, the point cloud is transformed into a 3D Computer-Aided Design (CAD) model. This model can then be imported into SolidWorks for further analysis and used to design the workpiece, which will be employed in the CMM to securely hold the blades during measurement.

#### 4.1.2 Mitutoyo Euro-C 121210

The CMM is a highly precise tool used to measure the geometry of parts and components. It works by using a probe that senses the physical contact with the object. While traditional CMMs rely on touch-trigger probes, there are other models that use laser or optical sensors to take measurements. The Mitutoyo Euro-C 121210 CMM is controlled by a computer and operates within a three-dimensional coordinate system.

This particular CMM is equipped with a Renishaw Revo-2, providing it with five degrees of freedom (DoF). In addition to moving along the three main axes, the machine can adjust the probe's angles, enabling it to measure even the most complex surfaces that would otherwise be difficult to reach. The machine setup includes a granite bed, probe, probe tree, arm, joystick, and specialized software, as shown in Figure 4.1.

Although four probes are available for use with the Renishaw Revo-2, only two are applicable to this project. Among them, the RSP2-3 is the sole probe that enables full five-degree-of-freedom operation. As illustrated in Figure 4.2, the first three DoFs (X, Y, and Z) are controlled by the CMM arm, while the remaining two ( $\alpha$ ,  $\beta$ ) are executed by the probe itself.

Each probe has distinct characteristics suited for different tasks, as detailed in Table 4.1.

Table 4.1: Renishaw probes available at TAP

Probe	DoF	Scanning Capability	Sphere Ø
RSP2-3	5	2D	6mm
RSP3	3	3D	4mm

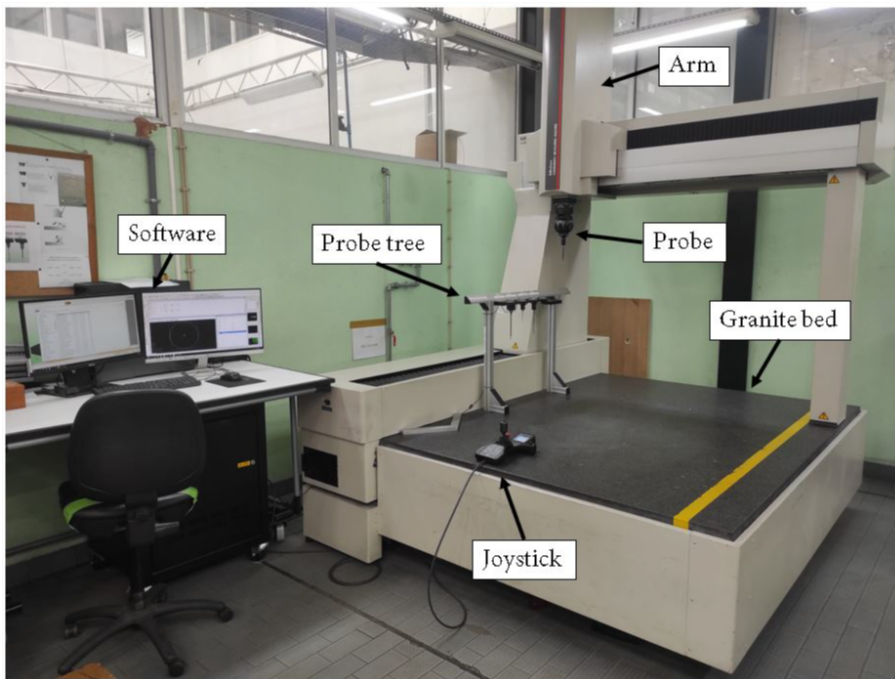


Figure 4.1: Mitutoyo Euro-C 121210 Components [14]

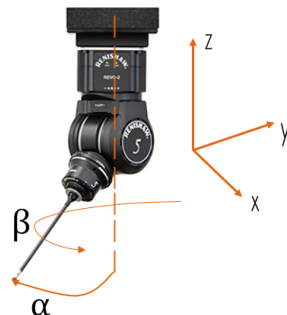


Figure 4.2: DOF of the Renishaw probe [13]

The integration of the CMM into this project plays a key role in ensuring that every high-pressure compressor rotor blade is measured quickly, accurately, and consistently. The development of a custom inspection program aims to enable the production team to measure entire sets of blades with minimal manual intervention, enhancing both efficiency and reliability.

Through the use of the CMM, it is possible to automatically verify critical dimensions, such as Chord Length (CL), Leading Edge Thickness (LET), Trailing Edge Thickness (TET), and overall airfoil geometry. This ensures that each blade meets the required tolerances while eliminating inconsistencies associated with manual measurement methods. Additionally, this automation reduces the workload of operators, allowing them to focus on other essential tasks while the machine performs the measurements.

Another significant advantage of the CMM is its ability to generate detailed inspection

reports, facilitating the tracking of blade conditions over time. This capability extends beyond simple compliance verification, contributing to predictive maintenance strategies that enhance engine performance and reduce unexpected maintenance costs.

By incorporating this level of automation and precision into the inspection process, the proposed approach aims to streamline production, improve quality control, and establish a more efficient and standardized methodology for [TAP](#)'s maintenance operations.

## 4.2 TAP ME: Previous Theses on Dimensional Inspection

In the past, several master's theses have been developed in collaboration with [TAP ME](#), contributing to the improvement of measurement and inspection processes for aircraft engine components. One of these studies was conducted by Farinha, E. [5], focusing on the design of a fixture and the development of a measurement method for high-pressure compressor (HPC) rotor blades. This research continued the work initiated by Rendas, P. [13], who laid the foundation for the development of a fixture specifically designed for HPC rotor blade inspection.

Additionally, Baptista, F. [12] contributed to this field by developing a model that predicts the off-design performance of the CFM56-5B turbofan engine. More recently, Guerreiro, A. [8] worked on the development of a process to measure the exit flow area of the low-pressure turbine (LPT) nozzles from the same engine model. His study focused on creating an automated program for Coordinate Measuring Machine (CMM) inspection, addressing a previously undeveloped process within [TAP ME](#)'s engine maintenance operations.

While previous studies have primarily focused on components of the CFM56-5B engine, this thesis aims to extend the dimensional inspection process to the HPC rotor blades of the LEAP-1A engine. One project involves developing an optimized CMM measurement program for assessing the blade chord to evaluate performance, utilizing data from the test bank. The second project focuses on measuring and controlling platform clearance to optimize the assembly process. These improvements, applied to both the LEAP and CFM engines, build on previous research, further advancing the continuous optimization of inspection methods to adapt to newer engine generations.

## Current Progress and Work Plan

The analysis of the operation of the Maintenance and Engineering Unit included a demonstration of the component scanning process and a session on the functionality of the CMM. Following this, the process through which blades go through maintenance was described in detail, as shown in Figure 5.1, outlining each step in the maintenance cycle.

Additionally, a collection of scrapped HPC blades from a LEAP-1A engine was carried out, involving the tracking of blades that had been discarded during previous maintenance activities. This collection enabled the scanning and dimensional comparison between a new and a worn blade, with the goal of analyzing the extent of blade degradation over time and understanding its potential impact on performance.

In parallel, work on test cell data analysis was initiated, aiming to develop a program to assess the impact of variations in sensor readings on the final engine **Exhaust gas temperature (EGT)** measurement. This analysis seeks to identify key parameters that influence test cell results and to understand how performance evaluation is carried out. By gaining deeper insights into these factors, it will be possible to facilitate future analyses of the impact of blade chord length variations on engine performance.

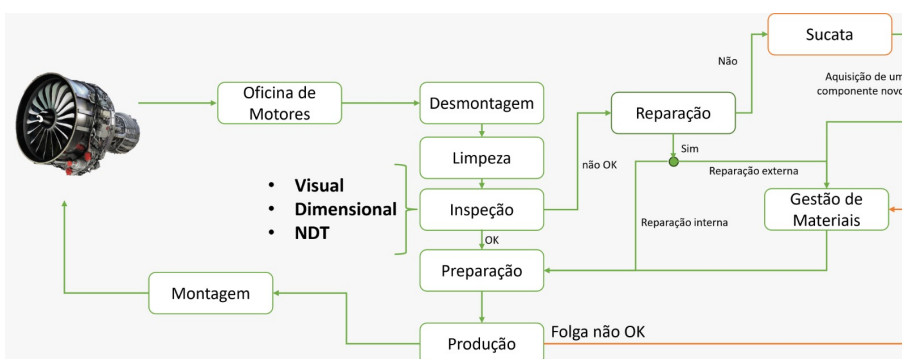


Figure 5.1: Process overview of blade maintenance cycle

## 5.1 Work Plan

To ensure a well-structured and efficient workflow, a provisional task plan has been created, as shown in Figure 5.2. The schedule will distribute key tasks over the coming months, allowing a balanced approach between research, development, and documentation. The initial phase focused on bibliographic research and drafting the dissertation introduction, providing a solid theoretical foundation. At the same time, work on scan processing and measurement tools will begin, setting the groundwork for later stages. Midway through the project, efforts will shift toward programming for chord measurement and analyzing test bench data—crucial steps for assessing engine performance. The final months will be dedicated to wrapping up the dissertation and completing the internship, ensuring all research components are properly integrated and documented. This structured approach is expected to help develop a project with practical value for the company while providing a highly enriching learning experience for the student.

	January	February	March	April	May	June	July	August	September
<b>Bibliographic Research</b>	Red	Red	Red	Red	Red	Red	Red	Red	Red
Introdução à Dissertação	Red	Red	White						
<b>Scan and Mesh Processing</b>	Light Gray	Red	Light Gray						
<b>Clearance Measurement Tool</b>	White	Red	Red	Red	Red	White	White	White	White
<b>Blade Fixation Tool</b>	Light Gray	Red	Red	Red	Red	Light Gray	Light Gray	Light Gray	Light Gray
<b>Programming for Chord Measurement</b>	White	White	White	Red	Red	Red	White	White	White
<b>Analysis of Test Bench Data</b>	White	White	White	White	White	Red	Red	Red	Red
<b>Conclusions and Dissertation Writing</b>	White	White	Red						
<b>Internship</b>	Light Gray	Red	Red	Red	Red	Red	Light Gray	Light Gray	Light Gray

Figure 5.2: Work Plan.

## Bibliography

- [1] K. Aainsqatsi. *Schematic Diagram of a 2-Spool, High-Bypass Turbofan Engine*. [Online; accessed 13-February-2025]. 2008-05. URL: [https://commons.wikimedia.org/wiki/File:Turbofan\\_operation.png](https://commons.wikimedia.org/wiki/File:Turbofan_operation.png) (cit. on p. 6).
- [2] *Brochure LEAP fiches 2017*. Brochure document. 2017 (cit. on pp. 6, 7).
- [3] A. Comercial. *Frota - TAP Air Portugal*. [Online; accessed 30-January-2025]. 2024-12. URL: <https://www.aviacaocomercial.net/frotatap.htm> (visited on 2024-12-01) (cit. on p. 3).
- [4] M. A. Engines. *LEAP-1A/-1B Commercial Aircraft Engines*. [Online; accessed 13-February-2025]. 2025. URL: <https://www.mtu.de/engines/commercial-aircraft-engines/narrowbody-and-regional-jets/leap-1a/-1b/> (cit. on p. 7).
- [5] E. E. Farinha and M. J. A. Santos. *Fixture Design and CMM Program Development for Measuring of High Pressure Compressor Rotor Blades*. Co-adviser: Mário Almeida Santos. 2021 (cit. on pp. 1, 22).
- [6] B. Fehrm. *Björn's Corner: New engine development. Part 22: High turbine technologies*. [Online; accessed 13-February-2025]. 2024-08. URL: <https://leehamnews.com/2024/08/30/bjorns-corner-new-engine-development-part-22-high-turbine-technologies/> (cit. on p. 8).
- [7] R. R. A. Group. *The Jet Engine*. Fifth. Rolls-Royce plc, 2007. ISBN: 0902121235 (cit. on pp. 4, 5, 12, 14, 16).
- [8] A. C. D. S. Guerreiro. *Development of a Process to Measure the Exit Flow Area of the Low Pressure Turbine Nozzle from the CFM56-5B Engine*. Thesis or internal report. N/A (cit. on p. 22).
- [9] J. M. Lourenço. *The NOVAtesis L<sup>A</sup>T<sub>E</sub>X Template User's Manual*. NOVA University Lisbon. 2021. URL: <https://github.com/joaomlourenco/novathesis/raw/master/template.pdf> (cit. on p. ii).

## BIBLIOGRAPHY

---

- [10] S. Metals. *INCONEL 718 Alloy*. [Online; accessed 06-February-2025]. url: <https://www.specialmetals.com/documents/technical-bulletins/inconel/inconel-alloy-718.pdf> (visited on 2025-02-06) (cit. on p. 16).
- [11] T. A. Portugal. *Manual de Manutenção Oficial LEAP1A - Hardware*. 2020 (cit. on pp. 8–11, 13, 15–17).
- [12] P. Rendas. *Fixture Design and Process Development for High Pressure Compressor Rotor Blades Measuring in Aircraft Engine Maintenance*. 2021, pp. 1–45 (cit. on p. 22).
- [13] Renishaw. *Renishaw: Enhancing Efficiency in Manufacturing and Healthcare*. <https://www.renishaw.com/en/renishaw-enhancing-efficiency-in-manufacturing-and-healthcare--1030>. Accessed: 2025-02-13. 2025 (cit. on p. 21).
- [14] L. Shi et al. “A Review on Leading-Edge Erosion Morphology and Performance Degradation of Aero-Engine Fan and Compressor Blades”. In: *Energies* 16 (7 2023-04), p. 3068. issn: 1996-1073. doi: [10.3390/en16073068](https://doi.org/10.3390/en16073068) (cit. on pp. 18, 21).
- [15] Trent1. *Axial Compressor and Turbine Operation*. <https://www.phase-trans.msm.cam.ac.uk/mphil/Trent1/sld011.htm>. Accessed: 2025-02-13. n.d. (Cit. on p. 11).



# THE MONTGOMERY COUNTY HIGH SCHOOL OF SCIENCE AND TECHNOLOGY

Montgomery County Public Schools

Montgomery County, Maryland

Montgomery County, Maryland